Oct 26th, 11:00 AM - 12:30 PM

NIR spectral signatures of flexor and extensor muscles of the upper and lower limb in humans at varying lengths

Antonio Curra
Sapienza University of Rome, antonio.curra@uniromal.it

Riccardo Gasbarrone
Sapienza University of Rome, riccardo.gasbarrone@uniromal.it

Giuseppe Bonifazi
Sapienza University of Rome, giuseppe.bonifazi@uniromal.it

NIR spectral signatures of flexor and extensor muscles of the upper and lower limb in humans at varying lengths

Antonio Currà [1], Riccardo Gasbarrone [2], Giuseppe Bonifazi [3], Silvia Srranti [3]

[1] Research Center for Biophotonics, Sapienza University of Rome, Polo Pontino, Italy
[2] Academic Neurology Unit, A. Fiorini Hospital, Terracina (LT), Department of Medical-Surgical Sciences and Biotechnologies, Sapienza University of Rome, Polo Pontino, Italy.
[3] Department of Chemical Engineering Materials Environment, Sapienza University of Rome, Italy

Abstract. NIR spectroscopy provides the spectral signatures (i.e. "fingerprints") of living human muscles, which represent specific, accurate, and reproducible measures of their overall biological status. We showed that chemometric analysis applied to NIR spectra acquired from the upper limb distinguishes the biceps from the triceps. We acquired muscles reflectance spectra in the Vis-SWIR regions (350-2500 nm), utilizing an ASD FieldSpec 4™ Standard-Res Spectroradiometer with a spectral sampling capability of 1.4 nm at 350-1000 nm and 1.1 nm at 1001-2500 nm. Optical spectroscopy proves effective for studying human muscles in vivo and contribute to non-invasive more thorough evaluation of the muscular system.

Keywords: Near Infrared Spectroscopy, muscles, limbs, muscle length.

Introduction

Nowadays, optical spectroscopy and chemometric modelling are widely used to perform both qualitative and quantitative analysis, not only because they are non- invasive and not destructive, but also because they are cost-effective, simple and quick to use. Near InfraRed Spectroscopy (NIRS) based techniques are widely utilized in primary and secondary raw materials sector [1 - 4], cultural heritage [5, 6], agricultural and food industry [7-12], pharmaceutical and chemical industry [13, 14], and analytical science [15]. The dramatic advancement of technology and device miniaturization contributes to continue the success of NIR-based investigation technique. NIR portable devices and/or HyperSpectral Imaging (HSI) systems have taken place in various quality control applications and logics. In clinical research and medical applications, NIRS has been successfully applied for different purposes: i.e. functional analysis of human tissues [16], evaluation of muscles oxygenation [17], microvascular function [18] and damage [19], and assessment of wounds [20] and cartilage [21]. We used NIRS to analyse human muscles in vivo [22-24]. The idea stemmed from studies in food science, showing that combined application to meats of NIR-based detection and chemometrics allows discrimination of lamb muscles [25], prediction of chemical constituents in lamb meats [26] and classification of fresh and frozen-thawed pork muscles [27, 28]. Muscle tissue has indeed optical properties suitable to be analyzed with spectroscopy [26-28], and we showed that NIRS proves a cheap, reliable, and widely applicable technique for non-invasive in vivo analysis of human muscles.

Aim of the present study is to apply NIR Spectroscopy technique and chemometric modelling for distinguishing muscles belonging to the upper or lower limb (biceps vs. triceps brachii vs. tibialis anterior vs. triceps surae); belonging to different functional groups (flexors vs. extensors); having different muscle length (short vs. long). A portable Vis-SWIR (Visible - Short Wave InfraRed) spectroradiometer, a device operating in the 350-2500 nm wavelength range, was used for collecting reflectance spectra from different muscles of the of upper limb (biceps and triceps brachialis) and lower limb (tibialis anterior and triceps surae) in normal subjects at varying lengths (long and short). Spectra pre- processing and Principal Component Analysis (PCA) were used for enucleating differences among the acquired reflectance spectra and for grouping the investigated muscles.

Methods and procedures

Vis-NIR analysis

Subjects enrollment, spectroradiometer device and spectra acquisition. Analyses were carried out collecting the spectral information of muscles of 10 Caucasian, southern European healthy subjects (age 24-89 years, 6 females). All study participants provided written consensus before being included in the study, approved by the institutional review board (Comitato Etico Lazio 2, protocol number 0167183/2018). All methods were carried out according to the relevant guidelines and regulations. Subjects anthropometric data are reported in Table 1.
Vis-SWIR (Visible - Short Wave InfraRed) reflectance spectra of the upper and lower limb muscles, in two different positions (short and long) were acquired by a portable spectroradiometer. Ten spectra in short and long position were collected using an ASD FieldSpec 4® Standard-Res unit, for: biceps, triceps brachialis (upper limb), triceps surae and tibialis anterior (lower limb) of each subject (800 spectra). Measurements were performed in fixed limb postures. The spectra collection was always performed by the same operator.

Table 1. Anthropometric data of enrolled subjects ("0 = male" and "1 = female").

ID	Age	Sex	Weight [kg]	Height [cm]
S1	51	0	80	173
S2	74	0	-	-
S3	44	1	65	-
S4	89	0	70	171
S5	29	1	45	-
S6	54	0	80	187
S7	49	1	59	169
S8	61	1	55	-
S9	24	0	74	167
S10	69	0	-	-

The spectroradiometer works in the spectral range 350 – 2500 nm and it has a spectral resolution of 3 nm at 700 nm and 10 nm at 1400/2100 nm [29, 30]. It essentially consists of a detectors case and a fiber optic cable with a contact probe, connected to a personal computer /

laptop. The system has different separate holographic diffraction gratings: a VNIR detector (350-1000 nm; 512 elements silicon array), a SWIR1 detector (1001-1800 nm; Graded Index InGaAs. Photodiode, Two Stage TE Cooled) and a SWIR2 detector (1801-2500 nm; Graded Index InGaAs. Photodiode, Two Stage TE Cooled). Order separation filters cover each detector for eliminating second and higher order light. While, the ASD Contact Probe (with a weight of 0.7 kg), allowing reflectance measurements, consists of a halogen bulb light source (color temperature of 2901
±10%°K) with a Field of View (FOV) of about 1 cm2. Native software of the ASD instrument, called RS3, have been used for data acquisition and handling [30].

Instrument calibration procedure and spectral data handling. Prior to spectra collection, the instrument was calibrated. The procedure of spectroradiometer calibration starts with dark acquisition (D_i) and the measurement of the "white reference" (W_i) material [31]. After this calibration stage, the spectra (R_{0i}) is acquired and the reflectance (R_i) is then computed, by using the Equation 1:

$$R_i = \frac{R_{0i} - D_i}{W_i - D_i} \quad (1)$$

Dark current was computed referencing the dark current calibration file. White reference was acquired on a Spectralon white reference standard from LabSphere™ (99% nominal reflectance). Calibration procedure was carried out using the ASD RS3 (Ver. 6) software. Data files were first converted into ASCII text files by the aid of ViewSpec Pro software (Ver. 6.2.0.) and then imported into MatLab® (The MathWorks, Inc.) environment (MATLAB R2016b; ver. 9.1.0.441655. Imported data files were analyzed using the Eigenvector Research, Inc PLS_toolbox (Ver. 8.2.1) operating inside the MatLab® environment. Data were stored into datasets objects and classes were set.

Chemometric analysis

Spectra pre-processing. The difference between spectra can be enhanced applying pre-processing algorithms to the acquired raw spectra. Data pre- processing of reflectance data is important also for removing un-wanted noise, due to light scattering and/or other physical phenomena [32]. In this scenario, different combinations of pre-processing algorithms were used. The selected combination of pre-processing used in this study is reported in the following: Extended Multiplicative Scatter Correction (EMSC), Generalized Least Square - Weighting (GLS-W) on classes to be explored (with $\alpha = 0.002$) and Mean Center (MC). EMSC was used for correcting scatter artifacts. While, GLS-W was applied to down-weight the difference or "clutter", inside classes. GLS-W consists of a multivariate filter, which calculates a filter matrix based on differences among groups of samples, which should otherwise be similar. Finally, mean centering was performed in order to remove the mean value from the data and to further enhance differences among samples.

Principal Component Analysis (PCA). The exploratory analysis of reflectance spectra data was performed by using Principal Component Analysis (PCA). PCA is a powerful chemometric tool that aim at gaining an in-depth understanding of the studied system. It gives the possibility to extract the dominants patterns of the reflectance spectral dataset matrix, in terms of the product of two smaller matrix of scores and loadings [33]. Thanks to this data decomposition method, it is thus possible to evaluate the samples structure and to easily identify patterns, such as clusters and/or outliers by simply graphically representing the position of all the samples in the Principal Components (PC) space (i.e. score plot). For every PCA performed, two PCs were chosen by exploring the eigenvalues plot.

Results and discussion

Reflectance spectra and exploratory analysis

Figure 1 shows raw spectra grand averages collected from biceps, tibialis anterior, triceps brachialis and triceps surae in each subject. Figure 2 shows raw spectra grand averages collected from all muscles belonging to the upper or lower limb. Figure 3 shows raw spectra grand averages collected from upper and lower limb muscles positioned at short and long fiber length. Figure 4 shows the grand averages of the raw spectra collected from all physiological flexors (i.e. biceps and tibialis anterior) and extensors (triceps brachialis and triceps surae).

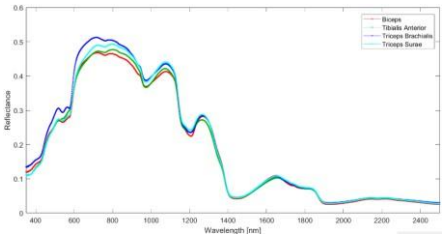

Fig. 1.

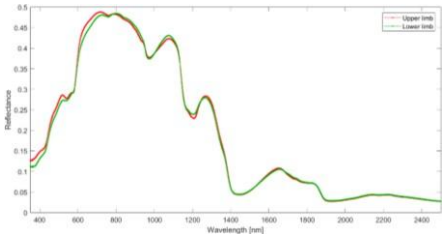

Fig. 2.

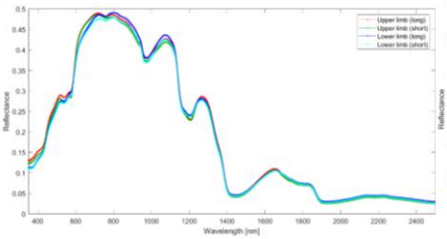

Fig. 3.

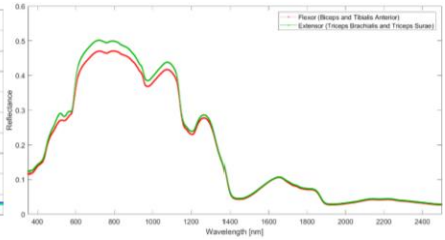

Fig. 4.

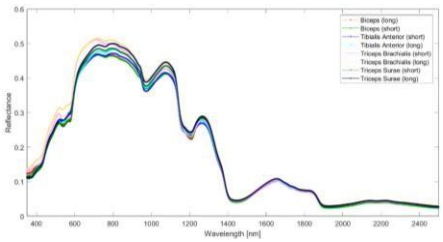

Fig. 5.

Figure 4 shows raw spectra the grand averages of all physiological flexors (i.e. bi- ceps and tibialis anterior) and extensors (triceps brachialis and triceps surae). Fig- ure 5 shows the grand averages of the raw spectra collected from biceps, tibialis anterior, triceps brachialis and triceps surae in short and long position.

The grand averages of reflectance spectra differ according to: i) the individual muscle from which spectra are acquired (Figure 1), ii) the limb to which the mus- cle from which spectra were acquired belongs to (Figure 2), iii) the length at which muscles were positioned when the

spectra were acquired (Figure 3), iv) the functional group to which muscle from which the spectra were acquired belong to (Figure 4) and, finally, v) the various features of the muscles from which the spec- tra were acquired (Figure 5). Differences in spectra can be seen around 760 nm, 970 nm, 1200 nm and at 1440 nm. Corresponding to adsorbing groups H2O o CH, CH2 (762 nm), H2O o CH (973), CH (1206 nm), H2O, CH, ROH, CONH2, CONHR (1442 nm), CH (1796 nm), H2O, RCO2R, CONH2 (1930 nm), RNH2,
CHC, CC (2186 nm) The peak wavelengths we found are similar to those reported
in studies about the classification of various animals meat cuts or meats [25-27].

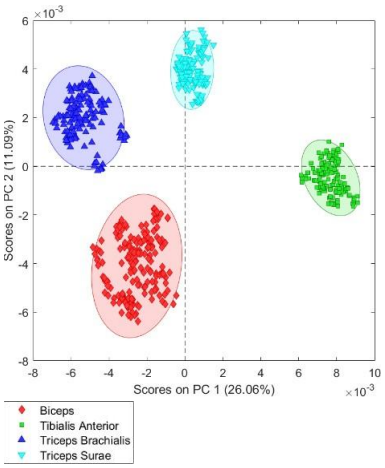

Fig. 6.

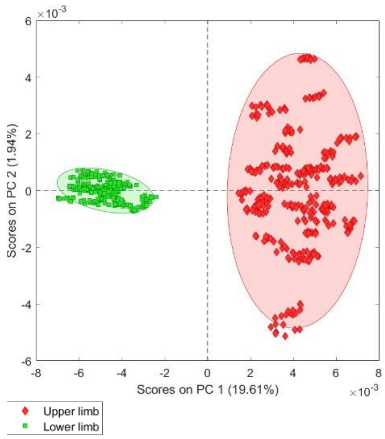

Fig. 7.

Differences among the set groups are explained by PCAs result. Figure 6 shows how the analyzed muscles groups in 4 different spaces of the scores plot. PC2 (11% captured variance) vs. PC1 (26% captured variance): i.e. biceps, tibialis an- terior, triceps brachialis and triceps surae. Figure 7 shows how muscles of the up- per (biceps and triceps brachialis) and lower (tibialis anterior and triceps surae) limb separate clearly in PCA analysis to form two distinct groups. Figure 8a shows the scores of the reflectance spectra for four classes: upper limb (short), up- per limb (long), lower limb (short) and lower limb (long). Along the scores on PC1 (20% of captured variance), upper limb and lower limb muscles are grouped in two sharply separated cluster. Along the scores on PC2 (2% of captured vari- ance), upper limb (short) group partially overlaps the upper limb (long) cluster. Reasonably, this finding refers to muscles dimension: upper limb muscles are “smaller” than lower limb muscles, therefore it is conceivably that in some sub- jects the long length of an upper limb muscle approximate the short length of a lower limb muscle. Spaces of the scores plot overlap also for lower limb (short) and lower limb (long) classes on the second and third quadrants, and upper limb (short and long), as reported in Figure 8b and Figure 8c. These results suggest that the optical properties distinguishing the spectra, as belonging to “upper or lower limb”, predominate on those reflecting the length of muscle. Figure 9 shows the results of the PCA aiming to group muscles according to their function: i.e. flexor (biceps and tibialis anterior) and extensor (triceps brachialis and triceps surae). PC1 (18% of captured variance) explains differences between the two classes. Re- sults suggests as muscles physiological properties can influence their optical prop- erties. Figure 10 shows the scores on PC 2 (10% of captured variance) vs. scores on PC 1 (30% of captured variance) for biceps, tibialis anterior, triceps brachialis and triceps surae in short and long positions. Muscles cluster in 4 areas of the scores plot.

Considering the length of the muscles, similarly as what seen in Fig- ure 8a, cluster of the single muscle partially overlaps (i.e. long and short).

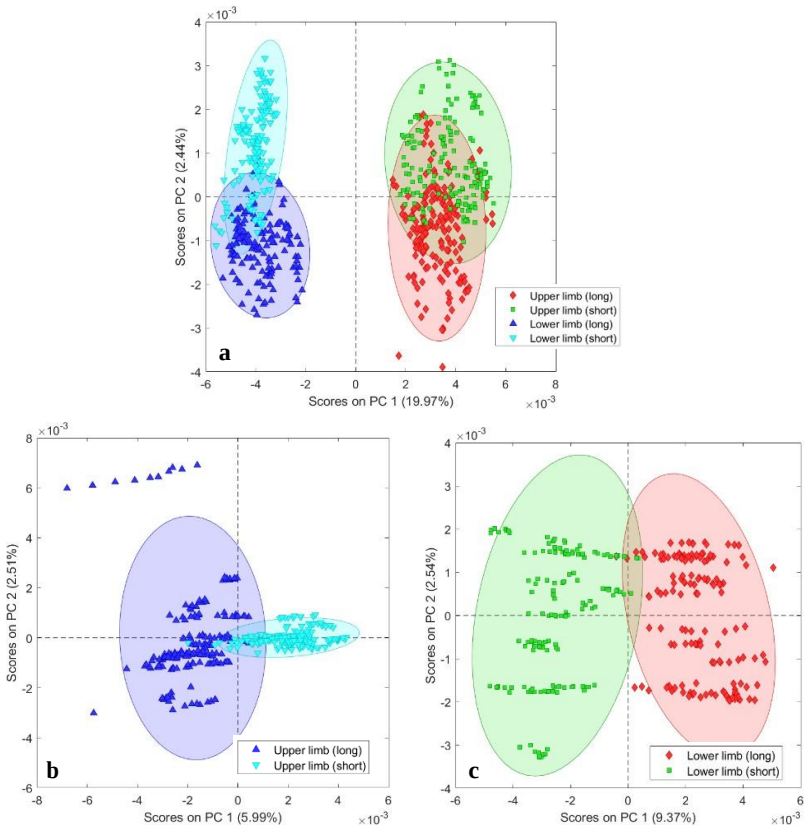

Fig. 8.

Conclusions

This study aimed to test whether NIR spectroscopy techniques can be utilized to study distinct characteristics of human muscles in vivo. We showed that distinct muscles have distinct spectral signatures, and they can be distinguished by PCA. NIR distinguishes very well the single muscle, muscles belonging to distinct func- tional groups or limbs. In contrast - and paradoxically - muscle length proves not a specific marker for categorizing muscle. We consider this result related to small differences in the “absolute muscle lengths” in the various classes (i.e. long upper limb muscles approximate he absolute length of short lower limb muscles”).

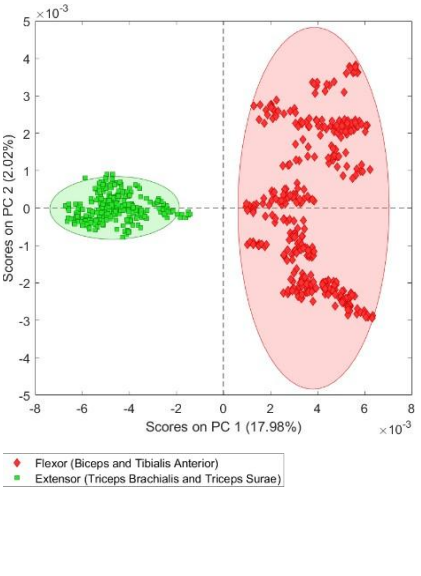

Figure 9.

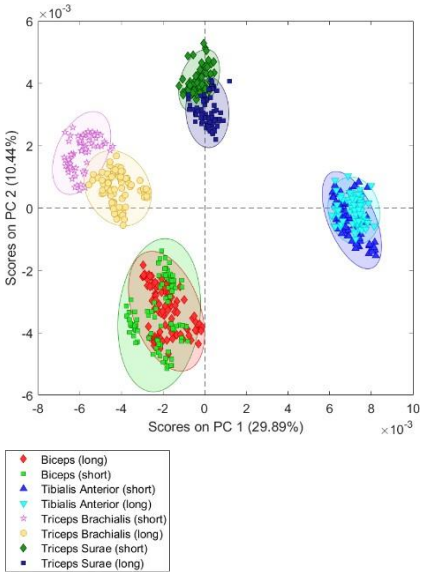

Figure 10.

The study confirms that NIR spectroscopy can be profitably applied to study human muscle tissue in vivo, and that Vis-SWIR reflectance spectra together with chemometric techniques allows to distinguished muscles (biceps vs. triceps bra- chii vs. tibialis anterior vs. triceps surae), and categorize them according to the limb (upper vs. lower) or the functional group (flexors vs. esxtensors) to which the muscle belongs. Further experiments are needed to test whether the optical proper- ties are related to the absolute length of the muscle. Further analysis in ongoing in order to calibrate and validate classification model aimed to test the effectiveness of the alleged prediction ability for the classes evaluated in this study and for se- lecting significant wavelengths.Due to the favorable properties of portable spec- trometers (i.e. size, rapidity of analysis and pain-free approach) and the clear find- ings reported, we conclude that NIR analysis may represent a new clinical/research tool addable to standard clinical investigation without significant cost and time penalties.

References

1. Masoumi, H., Safavi, S. M. and Khani, Z., “Identification and Classification of Plastic Resins using Near Infrared Reflectance Spectroscopy,” Int. J. of Mechanical, Aerospace, Industrial, Mechatronic and Manufacturing Engineering, 6(5), 877-884 (2012).
2. Bonifazi, G., Palmieri, R. and Serranti, S., “Hyperspectral imaging applied to end-of-life (EOL) concrete recycling,” tm-Technisches Messen, 82 (12), 616–624 (2015).
3.
4. Bonifazi, G., Palmieri, R. and Serranti, S., “Short wave infrared hyperspectral imaging for recovered post-consumer single and mixed polymers characterization”, Proc. SPIE/IS&T Electronic Imaging (2015).

5. Bonifazi, G., Capobianco, G. and Serranti, S., “Asbestos containing materials detection and classification by the use of hyperspectral imaging,” J. of Hazardous Materials 344, 981-993 (2018).
6. Capobianco, G., Prestileo, F., Serranti, S. and Bonifazi, G., “Hyperspectral imaging- based approach for the in-situ characterization of ancient Roman wall paintings,” Periodico di Mineralogia, Special issue (3A), 407-418. (2015).
7. Agresti, G, Bonifazi, G., Calienno, L., Capobianco, G., Lo Monaco, A., Pelosi, C., Picchio, R. and Serranti, S. Surface Investigation of Photo-Degraded Wood by Colour Monitoring, Infrared Spectroscopy, and Hyperspectral Imaging. J. of Spectroscopy, (2013).
8. Teixeira dos Santos, C. A., Lopo, M., N.M.J. Páscoa, R. and A. Lopes, J., “A Review on the Applications of Portable Near-Infrared Spectrometers in the Agro-Food Industry;” Applied Spectroscopy, 67, 11, 1215–1233 (2013).
9. Kumaravelu, C., and Gopal, A., “A Review on the applications of Near-Infrared Spectrometer and Chemometrics for the Agro-Food Processing Industries,” Proc. 2015 IEEE International Conference on Technological Innovations in ICT for Agriculture and Rural Development (2015).
10. Serranti, S., Bonifazi, G., Gasbarrone, R., "Olive fruit ripening evaluation and quality assessment by hyperspectral sensing devices", Proc. SPIE 10665, Sensing for Agriculture and Food Quality and Safety X, 106650R (15 May 2018).
11. Serranti, S., Bonifazi, G., Gasbarrone, R., "Kiwifruits ripening assessment by portable hyperspectral devices", Proc. SPIE 10665, Sensing for Agriculture and Food Quality and Safety X, 106650S (15 May 2018).
12. Bonifazi, G., Gasbarrone, R. and Serranti, S.,"Dried red chili peppers pungency assessment by visible and near infrared spectroscopy ", Proc. SPIE 10986, 109861S (14 May 2019.
13. Tsuchikawa, S. and Kobori, H., “A review of recent application of near infrared spectroscopy to wood science and technology,” J Wood Sci, 61, 213–220 (2015).
14. Roggo, Y., Chalus, P., Maurer, L., Lema-Martinez, C., Edmond, A. and Jent, N., “A review of near infrared spectroscopy and chemometrics in pharmaceutical technologies,” J. of Pharmaceutical and Biomedical Analysis, 44, 683–700 (2007).
15. [Larrechi, M.S., and Callao, M.P., “Strategy for introducing NIR spectroscopy and multivariate calibration techniques in industry,” Trends in Analytical Chemistry, 22, 10 (2003).
16. Pasquini, C., “Near Infrared Spectroscopy: Fundamentals, Practical Aspects and Analytical Applications,” J. Braz. Chem. Soc., 14, 2, 198-219 (2003).
17. Sakudo, A., “Near-infrared spectroscopy for medical applications: Current status and future perspectives,” Clinica Chimica Acta 455, 181-188 (2016).
18. Olivier, N., Boissière, J. Allart, E., Mucci, P., Tevenon, A., Daussin, F. and Tiffreau, V., “Evaluation of Muscle Oxygenation by Near Infrared Spectroscopy in Patients with Facioscapulohumeral Muscular Dystrophy,” Neuromuscolar Disorders 26, 47-55 (2016).
19. Jones S., Chiesa S.T., Chaturvedi N., D. Hughes A.D., “Recent Developments in Near-infrared Spectroscopy (NIRS) for the Assessment of Local Skeletal Muscle Microvascular Function and Capacity to Utilise Oxygen, “Artery Research 16, 25-33 (2016).
20. Chrzanowski, S.M., Batra, A., Lee-McMullen, B., Vohra, R.S., Forbes, S.C., Jiang, H., Vandenborne, K. and Walter G.A., “Near-Infrared Optical Imaging Noninvasively

21. Detects Acutely Damaged Muscle, “ The American J. of Pathology 186, 10 (2016).
22. Sowa, M.G. Kuo, W., Ko, A. C-T. and Armstrong, D. G., “Review of near-infrared methods for wound assessment,” J. of Biomedical Optics 21 (9), 091304 (September 2016).
23. Olumegbon, I. A., Oloyede, A. and Afara, I. O., “Near-infrared (NIR) spectroscopic evaluation of articular cartilage: A review of current and future trends,” Applied Spectroscopy Reviews, 52, 6, 541–559 (2017).
24. Currà, A., Gasbarrone, R., Cardillo, A., Trompetto, C., Fattapposta, F., Pierelli, F., Missori, P., Bonifazi, G. and Serranti S., Near infrared spectroscopy as a tool for in vivo analysis of human muscles. Scientific Reports 9, Article number: 8623 (2019).
25. Gasbarrone, R., Currà, A., Cardillo, A., Bonifazi, G. and Serranti S., "Near infrared spectroscopy of human muscles", Proc. SPIE 10489, 1048914 (21 February 2018).
26. G. Bonifazi, A. Cardillo, A. Currà, R. Gasbarrone, S. Serranti, "Near infrared spectroscopy as a tool for in vivo analysis of human muscles ", Proc. SPIE 10662, Smart Biomedical and Physiological Sensor Technology XV, 106620O (14 May 2018).
27. Kamruzzaman, M., ElMasry, G., Sun, D. and Allen, P. “Application of NIR hyperspectral imaging for discrimination of lamb muscles,” Journal of Food Engineering, 104, 332–340 (2011).
28. Pu, H., Sun, D., Ma, J., Liu, D. and Kamruzzaman, M., “Hierarchical variable selection for predicting chemical constituents in lamb meats using hyperspectral imaging,” Journal of Food Engineering, 143 44–52 (2014).
29. Ma, J., Pu, H., Sun, D., Gao, W., Qu, J. and Ma, K., “Application of VisNIR hyperspectral imaging in classification between fresh and frozen-thawed pork Longissimus Dorsi muscles,” Int. J. of Refrigeration 50, 10-18, (2015).
30. Pu, H.2, Suna, D. Ma, J. and Cheng, J., “Classification of fresh and frozen-thawed pork muscles using visible and near infrared hyperspectral imaging and textural analysis”, Meat Science 99, 81–88 (2015).
31. ASD Inc., “FieldSpec 4 Standard-Res Spectroradiometer,”
32. <https://www.asdi.com/products-and-services/fieldspec- spectroradiometers/fieldspec-4-standard-res> (2017).
33. ASD Inc., “FieldSpec® 4 User Manual, ASD Document 600979, Rev. D,” (June 2015).
34. <http://support.asdi.com/Document/FileGet.aspx?f=600000.PD F> (2015).
35. M. I. Jamaludin, A. N. Matori and K. Cho Myint, “Application of NIR to Determine Effects of Hydrocarbon Microseepage in Oil Palm Vegetation Stress” (2015).
36. Rinnan, Å., van den Berg, F. and Engelsen, S.B., “Review of the most common pre-processing techniques for near infrared spectra”, Trends in Analytical Chemestry, 28, 10 (2009).
37. Wold, S., Esbensen, K. and Geladi, P., “Principal Component Analysis,” Chemometrics and Intelligent Laboratory Systems, 2, 37-52 (1987).